

Bound entanglement in the set of Bell state mixtures of two qutrits

Reinhold A. Bertlmann* and Philipp Krammer†

*Faculty of Physics, University of Vienna,
Boltzmannngasse 5, A-1090 Vienna, Austria*

We investigate the entanglement properties of a three-parameter family of states that are part of the *magic simplex* of two qutrits, which is a simplex of states that are mixtures of maximally entangled two-qutrit *Bell states*. Using entanglement witnesses we reveal large regions of bound entangled and separable states.

PACS numbers: 03.67.Mn, 03.65.Ca, 03.65.Ta, 03.67.Hk

Keywords: entanglement, bound entanglement, entanglement witness, qutrit

Entangled states are the basic ingredients of quantum information and quantum communication. For pure states of any dimension and any number of particles it is easy to determine if a state is entangled or not, the property is revealed by its reduced density matrices (see, e.g., Ref. [1]). For mixed states, however, it is in general difficult to decide whether a given density matrix is entangled or separable. Since quantum mechanical states are in practice rather mixed than pure, one seeks for criteria to detect entanglement and separability. Additionally, entangled states can be classified according to their distillability – a state is called *distillable* if from many copies of the same not maximally entangled state we can distill fewer maximally entangled states with statistical local operations and classical communication (SLOCC). Interestingly, not all entangled states are distillable. For states of higher dimension than 2×2 and 2×3 , there exist states that are entangled but not distillable, so-called bound entangled states [2, 3, 4, 5, 6, 7]. Apart from being a mathematical oddity bound entangled states physically characterize a set of states that are an obstacle for quantum information processing tasks, since once a system evolved into a bound entangled state, there is no way to retain a maximally entangled state with SLOCC. Nevertheless, concerning their usefulness, bound entangled states are not equivalent to separable states since their entanglement can be “activated” when used together with distillable entangled states [4]. It is the intention of this paper to present a certain family of two-qutrit states that lie within the *magic simplex* [8] – this family reveals a high geometric symmetry, can be classified according to its entanglement properties and contains large regions of bound entanglement.

We consider a Hilbert-Schmidt space $\mathcal{A}_A \otimes \mathcal{A}_B$ of operators on the finite dimensional bipartite Hilbert space $\mathcal{H}_A \otimes \mathcal{H}_B$, with dimension $d_A \times d_B$, $D := d_A d_B$. States ρ (i.e. density matrices) are elements of $\mathcal{A}_A \otimes \mathcal{A}_B$ with the properties $\rho^\dagger = \rho$, $\text{Tr } \rho = 1$ and $\rho \geq 0$. A scalar product on $\mathcal{A}_A \otimes \mathcal{A}_B$ is defined by $\langle A, B \rangle = \text{Tr } A^\dagger B$ with $A, B \in \mathcal{A}_A \otimes \mathcal{A}_B$.

Two basic concepts in the context of entanglement detection are entanglement witnesses [9, 10, 11, 12, 13] and the PPT Criterion (positive partial transposition) [9, 14]. An entanglement witness A detects the entanglement of states due to the convexity of the set of separable states S : A state ρ is entangled iff there exists a Hermitian operator A such that

$$\langle \rho, A \rangle = \text{Tr } \rho A < 0, \quad (1)$$

$$\langle \sigma, A \rangle = \text{Tr } \sigma A \geq 0 \quad \forall \sigma \in S. \quad (2)$$

For a given state ρ it is easy to find operators that provide Eq. (1), but in general difficult to show Eq. (2). Nevertheless it proves useful in many cases. If there exists a separable state $\tilde{\sigma}$ for which $\text{Tr} \tilde{\sigma} A = 0$, then A is called *optimal entanglement witness*. Optimal entanglement witnesses correspond to hyperplanes given by $\text{Tr} \tilde{\sigma} A = 0$ which are tangent to the set of separable states S .

An operational criterion that is easy to apply is the PPT Criterion: A separable state σ stays positive under partial transposition, $\sigma^{T_B} := (\mathbb{1} \otimes T) \sigma \geq 0$. We call a state PPT that is positive under partial transposition, and NPT a state that is not. Note that the PPT criterion is a necessary criterion for separability [14], that means if a state ρ is NPT, it has to be entangled. But if it is PPT, this does not automatically imply that it is separable, this is true for dimensions 2×2 and 2×3 only [9]. Amazingly, entangled PPT states are not distillable, thus *bound entangled* [3, 5, 7]. Clearly the PPT Criterion cannot distinguish PPT entangled from separable states, therefore other entanglement criteria have to be used, e.g. the entanglement witness criterion, which is the method that we will apply in this paper.

In Ref. [13] we presented a method to detect bound entanglement that is based on a geometrical approach: Consider a line of states ρ_λ inside the convex set of the PPT states between a PPT state ρ_{PPT} and the maximally mixed state,

$$\rho_\lambda := \lambda \rho_{\text{PPT}} + \frac{(1-\lambda)}{D} \mathbb{1}_D, \quad 0 \leq \lambda \leq 1, \quad (3)$$

and an operator

$$C_\lambda = \rho_\lambda - \rho_{\text{PPT}} - \langle \rho_\lambda, \rho_\lambda - \rho_{\text{PPT}} \rangle \mathbb{1}_D. \quad (4)$$

The operator C_λ is constructed geometrically in such way that we have $\text{Tr} C_\lambda \rho_\lambda = 0$ and $\text{Tr} C_\lambda \rho_{\text{PPT}} < 0$ (here $\lambda < 1$, the limit $\lambda \rightarrow 1$ is discussed later on). It divides the whole state space into states ρ_n for which $\text{Tr} C_\lambda \rho_n < 0$ and states ρ_p for which $\text{Tr} C_\lambda \rho_p \geq 0$, see Ref. [15]. If C_λ is an entanglement witness then all states ρ_n on one side of the plane are entangled. For a particular entanglement witness $C_{\tilde{\lambda}}$ all states ρ_λ are PPT and entangled for $\tilde{\lambda} < \lambda \leq 1$, thus bound entangled. Clearly the difficulty of the presented method lies in proving that $C_\lambda \geq 0 \forall \sigma \in S$. Different lines (3) are distinguished by different “starting states” ρ_{PPT} which will be called “starting points” throughout this text.

Next we apply the above method to a three-parameter family of the magic simplex of two qutrits. The magic simplex \mathcal{W} of bipartite qutrits (dimension 3×3) is introduced in Ref. [16], extended to qudits (dimension $d \times d$) in Ref. [8], reviewed and discussed in Ref. [6]. It is defined as the set of all states that are a mixture of *Bell states* P_{nm} ,

$$\mathcal{W} := \left\{ \sum_{n,m=0}^{d-1} q_{nm} P_{nm} \mid q_{nm} \geq 0, \sum_{n,m} q_{nm} = 1 \right\}, \quad (5)$$

where

$$P_{nm} := (U_{nm} \otimes \mathbb{1}) |\phi_d^+\rangle \langle \phi_d^+| (U_{nm}^\dagger \otimes \mathbb{1}). \quad (6)$$

The vector state $|\phi_d^+\rangle$ denotes the maximally entangled state $|\phi_d^+\rangle = \frac{1}{\sqrt{d}} \sum_j |j\rangle \otimes |j\rangle$ and the *Weyl operators* $U_{nm} = \sum_{k=0}^{d-1} e^{\frac{2\pi i}{d} kn} |k\rangle \langle (k+m) \bmod d|$ form an orthogonal basis $\{U_{nm}\}$ ($n, m = 0, 1, \dots, d-1$) of the Hilbert-Schmidt space [17, 18].

The indices n and m can be viewed as coordinates in a discrete phase space, and the points for fixed n or m constitute lines within. The magic simplex is highly symmetric and exhibits the same geometry under a line change (for details see Refs. [6, 16]). It thus represents the

eight-dimensional analogue of the three-dimensional simplex, a tetrahedron, of two-qubits which is the set of states that are mixtures of the four two-qubit Bell states [12, 19, 20, 21]. The two-qudit Bell states (6) play an important role in extensions of quantum communication procedures to higher dimensional systems – e.g. in the quantum teleportation protocol [17]. They constitute the corresponding maximally entangled orthogonal basis and the Weyl operators U_{nm} are a generalization of the Pauli operators, in the sense that Bob has to apply one of the d^2 operators (including the identity operator) to obtain the teleported state.

We want to consider a three-parameter family of states, introduced in Ref. [13], of the magic simplex that are a mixture of the maximally mixed state and two phase space lines,

$$\rho_{\alpha,\beta,\gamma} := \frac{1 - \alpha - \beta - \gamma}{9} \mathbb{1} + \alpha P_{00} + \frac{\beta}{2} (P_{10} + P_{20}) + \frac{\gamma}{3} (P_{01} + P_{11} + P_{21}). \quad (7)$$

The parameters are constrained by the positivity requirement $\rho_{\alpha,\beta,\gamma} \geq 0$, which results in $\alpha \leq 7\beta/2 + 1 - \gamma$, $\alpha \leq -\beta + 1 - \gamma$, $\alpha \leq -\beta + 1 + 2\gamma$, and $\alpha \geq \beta/8 - 1/8 + \gamma/8$. The constraints geometrically represent a pyramid with triangular base, see Fig. 1. The PPT Criterion selects those points (α, β, γ) that correspond to positive operators when subjected to partial transposition. We obtain the constraints $\alpha \leq -\beta - 1/2 + \gamma/2$, as well as $\alpha \leq (-2 + 11\beta - \gamma + 3\sqrt{\Delta})/16$ and $\alpha \leq (-2 + 11\beta - \gamma - 3\sqrt{\Delta})/16$, where we defined $\Delta = 4 + 9\beta^2 + 4\gamma - 7\gamma^2 - 6\beta(2 + \gamma)$, which form a cone that intersects the pyramid, and in the intersection region lie the PPT states, see Fig. 1.

A parameterized line of states $\rho_{\alpha,\beta,\gamma}$ situated on the boundary plane $\alpha = 7\beta/2 + 1 - \gamma$ (which we will from now on refer to as the *boundary plane*) is given by

$$\rho_b \equiv \rho_{\alpha,\beta,\gamma} \quad \text{with} \quad \alpha = \frac{6-b}{21}, \quad \beta = -\frac{2b}{21}, \quad \gamma = \frac{5-2b}{7}, \quad (8)$$

which exactly corresponds to the states

$$\rho_b = \frac{2}{7} |\phi_+^3\rangle \langle \phi_+^3| + \frac{b}{7} \sigma_+ + \frac{5-b}{7} \sigma_-, \quad 0 \leq b \leq 5 \quad (9)$$

that were introduced in Ref. [4]. We call this one-parameter family *Horodecki states* or *Horodecki line*. It is shown in Ref. [4] that these states are entangled for $4 < b \leq 5$, bound entangled for $3 < b \leq 4$ and separable for $2 \leq b \leq 3$. For convenience we express the parameter b in terms of γ to obtain a parametrization of the Horodecki line with γ .

In Ref. [13] we discovered planar regions of bound entanglement that go beyond the Horodecki line with the method discussed before, where the starting points ρ_{PPT} of the line ρ_λ (3) are chosen as the bound entangled Horodecki states. The inequality (2) is proven by expressing the operator C_λ and the separable states in terms of Weyl operator tensor products. In this way we arrive at a sufficient condition for C_λ such that Eq. (2) is satisfied:

Lemma 1. *For any Hermitian operator C of a bipartite Hilbert-Schmidt space of dimension $d \times d$ that is of the form*

$$C = a \left((d-1) \mathbb{1}_{d^2} + \sum_{n,m=0}^{d-1} c_{nm} U_{nm} \otimes U_{-nm} \right), \quad a \in \mathbb{R}^+, \quad c_{nm} \in \mathbb{C} \quad (10)$$

the expectation value for all separable states is positive,

$$\langle \rho, C \rangle \geq 0 \quad \forall \rho \in S, \quad \text{if} \quad |c_{nm}| \leq 1 \quad \forall n, m. \quad (11)$$

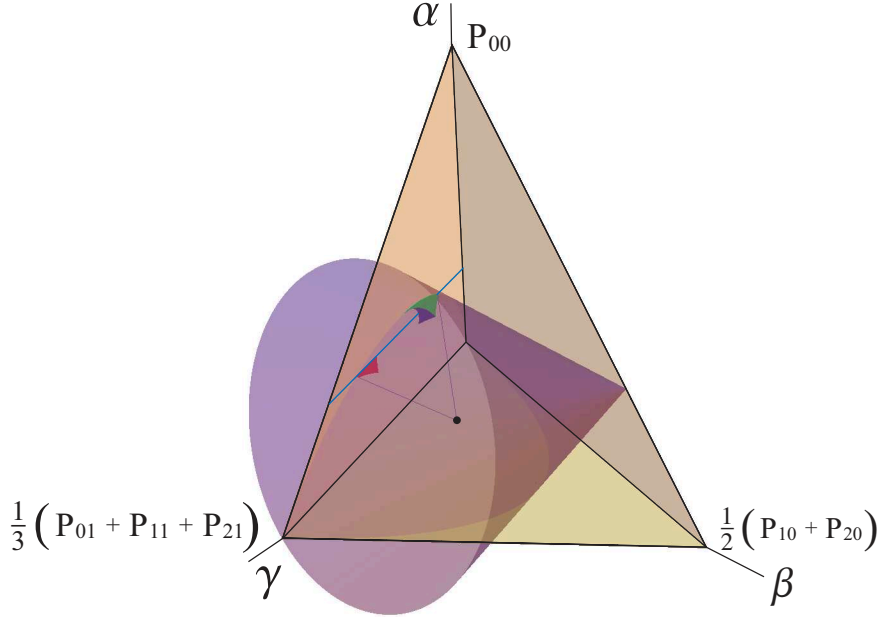


FIG. 1: (Color online) In the parameter space representing the Hilbert-Schmidt space geometry the states $\rho_{\alpha,\beta,\gamma}$ (7) lie inside a pyramid with triangular base, the PPT points form a cone. The intersection region includes the PPT states, i.e. separable and bound entangled states. The maximally mixed state is represented by the black dot. The line (blue) on the boundary plane indicates the Horodecki states (9), the planar section (red) jutting out of the Horodecki line shows the bound entangled states that are detected using starting points on the Horodecki line only. The protruding volume (blue/green) is the volume of bound entangled states that can be obtained with starting points deviating from the Horodecki line. In fact the picture is symmetrical for positive and negative values of γ , but for the sake of clarity only one volume is depicted. All parameter axes are chosen non-orthogonal to each other such that they become orthogonal to the boundary of the positivity region in order to reproduce the symmetry of the magic simplex.

If we choose the starting points not only on the Horodecki line, but also in a neighborhood of the line on the boundary plane, we can detect volumes of bound entanglement, see Fig. 1. These starting points ρ_{plane} are parameterized with an additional parameter ϵ that accounts for the amount of deviation from the line,

$$\rho_{\text{plane}} \equiv \rho_{\alpha,\beta,\gamma} \quad \text{with} \quad \left(\alpha = \frac{1 + \gamma + \epsilon}{6}, \beta = \frac{-5 + 7\gamma + \epsilon}{21}, \gamma \right), \quad \epsilon \in \mathbb{R}. \quad (12)$$

The parameters ϵ and γ of the states ρ_{plane} are restricted by the condition $|c_{nm}| \leq 1 \forall n, m$ of Lemma 1. The coefficients $c_{nm}(\gamma)$ of C_λ fulfil $c_{nm}(\gamma) = c_{nm}^*(-\gamma)$, hence Lemma 1 can be applied for positive and negative values of γ , and we obtain a symmetric picture. We restrict ourselves to positive values of γ , obtaining the “negative side” by applying $\gamma \rightarrow -\gamma$. The starting points on the plane can be seen in Fig. 1 as the points where the volumes of bound entangled states emerge from the boundary plane. Note that only the states inside the volumes are bound entangled for sure, states $\rho_\lambda^{\text{surface}}$ on the surface can be either separable or bound entangled. The reason is that for points $\rho_\lambda^{\text{surface}}$ we have $\text{Tr} \rho_\lambda^{\text{surface}} C_\lambda^{\text{surface}} = 0$ and in general we do not know whether the operator $C_\lambda^{\text{surface}}$ defines a tangent plane to the

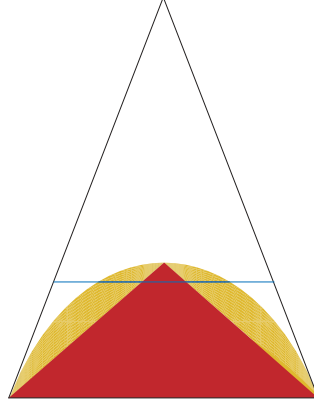


FIG. 2: (Color online) The entanglement properties of states $\rho_{\alpha,\beta,\gamma}$ on the boundary plane $\alpha = (7/2)\beta + 1 - \gamma$. The separable states are situated in the triangular region (red), the PPT entangled (bound entangled) states lie in between the triangular and parabolic region (orange), and the remaining states are NPT entangled. Interestingly, the Horodecki line (blue) runs through all entanglement characteristics.

set of separable states, i.e. whether it is already optimal. The detected regions of bound entanglement, the “old” planar region and the “new” volumes, are plotted in Fig. 1.

Entanglement witnesses of the form (4) correspond to planes in our three-dimensional illustration of the Hilbert-Schmidt space. They detect not only the entanglement of states on lines ρ_λ (3), but also of all states lying on the same side of the plane that includes the starting points ρ_{PPT} of ρ_λ . Consider for example a starting point ρ_{plane}^1 (12) on the boundary plane that represents the lower tip of the bound entangled volume in Fig. 1, it is given by $(\epsilon = -1/4, \gamma = 1/4)$. Using Lemma 1 we find that for ρ_{plane}^1 the operator $C_1 := C_\lambda/\lambda(1 - \lambda)$ is an entanglement witness for $\lambda \rightarrow 1$ and has a simple matrix form which we can easily calculate from Eq. (4).

Now we explain how to detect further bound entangled states and the region of separability. The trace $\text{Tr } C_1 \rho_{\text{plane}}^1 = 0$ provides the plane equation $Pl_1 : \alpha = 2(1 + 2\beta - \gamma)/5$. Plane Pl_1 intersects the boundary plane on the line $l_a : \beta = 2(-1 + \gamma)/9$, the cone of PPT states intersects the boundary plane on the curve $l_b : \beta = (-4 + 3\gamma + \sqrt{4 - 3\gamma^2})/9$, and l_a and l_b cross each other at $\gamma = 0$ and $\gamma = 1$. These crossing points are separable states: $\gamma = 0$ corresponds to two-parameter states [13, 16], in this case it is proved in Ref. [16] that all PPT states are separable, and for $\gamma = 1$ we have $\alpha = \beta = 0$, i.e. an equal mixture of the Bell states P_{01} , P_{11} , and P_{21} , which is separable too [16]. The hyperplane of the entanglement witness cuts the boundary plane at the line l_a , it contains two separable states, therefore it represents an optimal entanglement witness that has to be tangent to the set of separable states S . Since S is convex the line l_a has to describe the boundary of the separable states between $\gamma = 0$ and $\gamma = 1$. Therefore the whole region between l_a and l_b has to be bound entangled, it is given by $0 < \gamma < 1$, $2(-1 + \gamma)/9 < \beta < (-4 + 3\gamma + \sqrt{4 - 3\gamma^2})/9$ and $\alpha = 7\beta/2 + 1 - \gamma$. For the Horodecki states we thus find bound entanglement for $1/7 < \gamma \leq 3/7$ and separability for $0 \leq \gamma \leq 1/7$, which (for $\gamma \rightarrow -\gamma$) recovers the result of Ref. [4]. The regions of separable, PPT entangled and NPT entangled states on the boundary plane are illustrated in Fig. 2.

The plane Pl_1 representing the entanglement witness also intersects the PPT cone inside

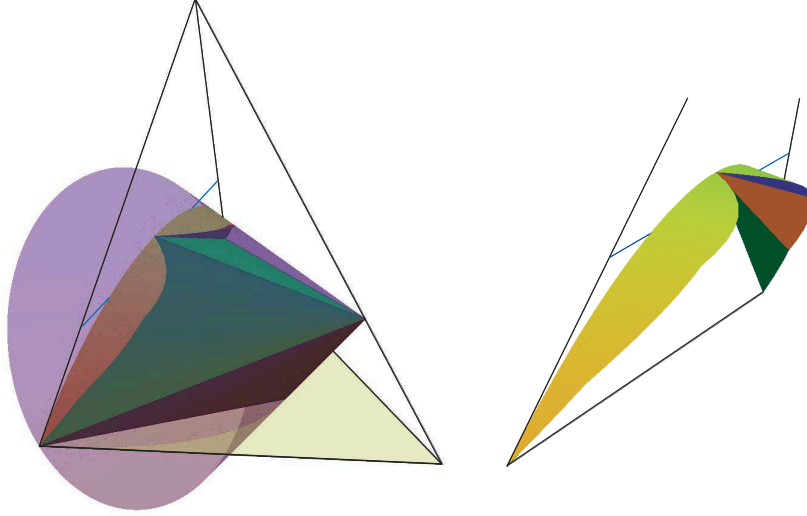


FIG. 3: (Color online) Right: The detected regions of bound entanglement extending from the boundary plane (enlarged) as intersections of the planes Pl_1 (green), Pl_2 (red) and Pl_3 (blue) (from bottom to top) corresponding to three entanglement witnesses. Left: The polygon (green) encloses the states that are necessarily separable. In between the polygon and the surface of the PPT cone lie the detected volumes of bound entanglement.

the pyramid; thus the bound entangled states extend from the boundary plane into the volume. The region of bound entanglement is then confined by the surface of the PPT cone $\alpha = (-2 + 11\beta - \gamma + 3\sqrt{\Delta})/16$, the plane Pl_1 , and the boundary plane.

We can detect regions of bound entanglement that reach even further into the pyramid by using other entanglement witnesses that correspond to other planes intersecting the cone. We construct again witnesses with our geometric method on lines starting on the boundary plane around the Horodecki line and such we obtain the smallest possible value of λ , i.e., $\lambda_{\min}^{\text{tot}} = (3 + \sqrt{13})/8 \simeq 0.826$, for the starting point with $\epsilon_0 = (-25 + 7\sqrt{13})/2 \simeq 0.12$ and $\gamma = \sqrt{5 + 11\epsilon_0/3 - 5\epsilon_0^2/12}/7 \simeq 0.35$. The state on this line with $\lambda_{\min}^{\text{tot}}$ is the outermost point of the bound entangled volume (the green tip in Fig. 1) that reaches into the PPT cone. The entanglement witness C_λ corresponding to $\lambda_{\min}^{\text{tot}}$ gives the plane equation $Pl_2 : \alpha = (-524 + 148\sqrt{13})^{-1}[16(-7 + 2\sqrt{13}) - 4(-5 + \sqrt{13})\beta + (-94 + 26\sqrt{13} + 3(-5 + \sqrt{13})\sqrt{2\epsilon_0})\gamma]$. It offers a new boundary for the bound entangled region that extends further into the pyramid (but detects fewer bound entangled states on the boundary plane of the pyramid). A final extension we find by considering the line that starts at a point $\gamma = 2/7$ of the intersection curve of Pl_1 with the PPT cone. The minimal λ such that C_λ (4) represents an entanglement witness according to Lemma 1 is $\lambda_{\min} = 7(2328 + 331\sqrt{39})/32763 \simeq 0.94$, and the corresponding plane $Pl_3 : \alpha = (150 - 18\sqrt{39})^{-1}[24 - 2\sqrt{39} + (-42 + 9\sqrt{39})\beta - 6(-5 + \sqrt{39})\gamma]$ provides a new boundary for the bound entangled states reaching yet a bit further into the volume of the pyramid. The planes Pl_1, Pl_2, Pl_3 together with the detected volumes of bound entangled states we have depicted in Fig. 3.

Naturally the question arises if we can detect all regions of NPT entangled, PPT entangled and separable states for our three-parameter family of states (7). As a first step to an answer we can identify a polygon of states that have to be separable for sure by connecting

all outermost separable states we know so far in a convex manner. These known states are the boundary of the PPT states for $\gamma = 0$, which form a trapezoid, and the boundary of the separable states on the boundary plane. The resulting polygon can be seen in Fig. 3.

Numerical calculations imply that the set of separable states is larger than the constructed polygon, and that bound entanglement is mainly concentrated in the region we detected. These results require numerical minimizations to obtain the needed entanglement witnesses, and the detailed procedure will be discussed in a forthcoming article.

Summarizing, we find new, large regions of bound entangled states in a three-parameter family of the magic simplex of two qutrits. We detect the definite regions of separable, PPT entangled and NPT entangled states on a boundary plane of the family of states by using entanglement witnesses that are constructed geometrically. The regions of bound entangled states extend from the plane into the pyramid of the states forming such large volumes of bound entanglement that include the Horodecki states as a small line. Finally, we construct a convex subset of the three-parameter family, a polygon, that encloses states that are necessarily separable.

We would like to thank Alexander Ableitinger for helpful comments. This research has been financially supported by the FWF project CoQuS No W1210-N16 of the Austrian Science Foundation and by the F140-N Research Grant of the University of Vienna.

* Electronic address: reinhold.bertlmann@univie.ac.at

† Electronic address: philipp.krammer@univie.ac.at

- [1] D. Bruß, *J. Math. Phys.* **43**, 4237 (2002).
- [2] P. Horodecki, *Phys. Lett. A* **232**, 333 (1997).
- [3] M. Horodecki, P. Horodecki, and R. Horodecki, *Phys. Rev. Lett.* **80**, 5239 (1998).
- [4] P. Horodecki, M. Horodecki, and R. Horodecki, *Phys. Rev. Lett.* **82**, 1056 (1999).
- [5] E. M. Rains, *Phys. Rev. A* **60**, 179 (1999).
- [6] B. Baumgartner, B. C. Hiesmayr, and H. Narnhofer, arXiv:0705.1403.
- [7] R. Horodecki, P. Horodecki, M. Horodecki, and K. Horodecki, quant-ph/0702225.
- [8] B. Baumgartner, B. C. Hiesmayr, and H. Narnhofer, *J. Phys. A: Math. Theor.* **40**, 7919 (2007).
- [9] M. Horodecki, P. Horodecki, and R. Horodecki, *Phys. Lett. A* **223**, 1 (1996).
- [10] B. M. Terhal, *Phys. Lett. A* **271**, 319 (2000).
- [11] B. M. Terhal, *Theoretical Computer Science* **287**, 313 (2002).
- [12] R. A. Bertlmann, H. Narnhofer, and W. Thirring, *Phys. Rev. A* **66**, 032319 (2002).
- [13] R. A. Bertlmann and P. Krammer, *Phys. Rev. A* **77**, 024303 (2008).
- [14] A. Peres, *Phys. Rev. Lett.* **77**, 1413 (1996).
- [15] R. A. Bertlmann, K. Durstberger, B. C. Hiesmayr, and P. Krammer, *Phys. Rev. A* **72**, 052331 (2005).
- [16] B. Baumgartner, B. C. Hiesmayr, and H. Narnhofer, *Phys. Rev. A* **74**, 032327 (2006).
- [17] C. H. Bennett, G. Brassard, C. Crépeau, R. Jozsa, A. Peres, and W. K. Wootters, *Phys. Rev. Lett.* **70**, 1895 (1993).
- [18] H. Narnhofer, *J. Phys. A: Math. Gen.* **39**, 7051 (2006).
- [19] M. Horodecki and R. Horodecki, *Phys. Rev. A* **54**, 1838 (1996).
- [20] K. G. H. Vollbrecht and R. F. Werner, *Phys. Rev. A* **64**, 062307 (2001).
- [21] R. A. Bertlmann and P. Krammer, arXiv:0706.1743.